SEMARAK ILMU PUBLISHING

Journal of Advanced Research in Applied Sciences and Engineering Technology

Journal homepage:
https://semarakilmu.com.my/journals/index.php/applied_sciences_eng_tech/index
ISSN: 2462-1943

Analysis of Impedance Based Sensor to Discover the Invasive Nature of A549 Lung Cancer Cell

Muhammad Mahbubur Rashid[1,*], Mohamad Farhan Abd Razak[1], Tahsin Fuad Hasan[1]

[1] Department Mechatronics Engineering, Kulliyyah of Engineering, International Islamic University, Jalan Gombak, 53100 Kuala Lumpur, Malaysia

ARTICLE INFO

Article history:
Received 9 April 2023
Received in revised form 28 September 2023
Accepted 9 November 2023
Available online 20 March 2024

Keywords:

Impedance based sensor; ECIS; Invasive nature; Equivalent circuit model; Lung cancer cell; Quadratic equation

ABSTRACT

Numerous studies have been conducted to investigate the effectiveness of impedance-based sensors in detecting the invasive behaviour of cancer cells, specifically through the use of Electric Cell-substrate Impedance Sensing (ECIS) methodology. However, the current equivalent circuit models used to represent the invasive nature of cancer cells have limitations and inaccuracies, and there has been a lack of utilization of mathematical and data analysis software to better understand the growth and invasive behaviour of these cells. To address these gaps, this research aims to measure the impedance of A549 lung cancer cells, develop a simplified equivalent circuit model, and analyse the results using mathematical and data analysis software. The invasive behaviour of A549 cells will first be studied through impedance measurements, and then a circuit model will be designed and simulated using software tools to reveal the true invasive nature of these cells. Finally, rigorous mathematical analysis and the use of suitable data analysis software (such as Matlab Powergui and Simulink, EIS Spectrum Analyzer, and Plotly) will be applied to gain a comprehensive understanding of the morphological behaviour of the cells. The experimental results of this research are expected to align with previous findings, and a quadratic equation will be derived to predict the body's resistance of the A549 lung cancer cell using mathematical and data analysis approaches.

1. Introduction

In recent times, the impedance based sensor has been widely used in electrical and chemical engineering, and especially in biomedical field. Application of impedance measurement approach has been used for characterization of the DNA, for monitoring of the drug delivery, in the enhanced detection and characterization of adherent cells, in vitro biological applications, and in the discovery of tumor cells and the detection of cancerous cells. Moreover, the impedance based sensor measurement approach is an alternative method in the field of cancer research and is extremely useful in observing the growth of various cancer cells in terms of the cell's resistance and reactance. Besides that, the impedance bio-sensing approach which known as Electric Cell-substrate Impedance

* *Corresponding author.*
E-mail address: mahbub@iium.edu.my

https://doi.org/10.37934/araset.41.2.238255

Sensing (ECIS) is very accurate in terms of the sensitivity to the change of the environment. Furthermore, the impedance based sensor provides fast, label-free, quantitative measurement [11, 28].

Giaever *et al*., [16] has introduced impedance based sensor in the early 1980s. According to them, the fundamental setup of ECIS instrumentation uses standard tissue culture medium as the electrolyte, the ECIS electronics delivers a constant current to the electrodes while measuring the voltage and phase as a function of time. To ensure that the ECIS measurement is non-invasive, the current is maintained at a very low level. This low level AC current creates a very slight hyper- and hypo-polarization of the plasma membranes and has no measurable effect on the cell's behavior. The impedance is interpreted as a pure resistor and capacitor coupled in series and parallel combination [15].

As the field of ECIS is growing steadily, the National Foundation for Cancer Research recognizes the application of this approach in the cancer detection. The idea is to apply the ECIS measurement in detecting the potential of metastatic cells growth. Jiang [18] and Keese *et al*., [20] explained the possibility of cancer detection in the following experiment. There are three samples of HUVEC (human umbilical vein endothelial cells); the first sample act as the control without the cancer cells while the other two are challenged with highly metastatic AT3 subline and weakly G rat prostate cancer cell subline. The impedance is the electrical characteristic of any material. In a biological specimen it is known as the bio-impedance. For any biological specimen, the impedance consists of resistance and reactance. The reactance component only responds to AC supply while the resistance component is able to respond to both DC and AC supply. The electrical impedance (Z) is defined by two fundamental properties which are Resistance (R) and Reactance (X_c). The Resistance R component is passive and independent to the change of frequency while Reactance Xc component is active and dependent on the change of frequency. This can be seen in following equation; $X_c = 1/2\pi fC$. The value of impedance can be expressed as $Z = R + jX_c$. Besides that, the impedance is also defined as $Z = |Z|e^{j\theta}$ in polar form, where magnitude $|Z|$ denotes the ratio of voltage and current amplitudes while the θ denoted the phase difference between voltage and current [4].

The ECIS is a reliable and useful method for the detection of the cancer cells and to study the cell's nature and changes at different stages of the cancer's invasion by simply measuring the resistance and reactance values. Basically, for any equivalent circuit model, there are certain important variables that consist of resistors and capacitors. The whole impedance of this equivalent circuit model can be found by using simple mathematical equations after all the variables are calculated. Some of the common variables are:

1.1 Double Layer Capacitance (C_{dl})

Fairuzabadi [11] and Price [30] stated that this capacitance variable exists on the surface between the electrodes with its surrounding electrolyte. He also mentioned that two existing charges are incapable to connect with one another due to the small gap on the surface of the electrodes which acts as an insulator. The first one is the charged electrode while the other one is charged ions within the electrolyte.

1.2 Charge Transfer Resistance (R_{ct})

This resistance variable is formed due to a single kinetically-controlled electrochemical reaction which is caused by the immersion of the metal into the electrolyte [11]. Then, the metal will gradually

dissolve into the electrolyte forming ions and then the charged ions are transferred [11,32]. If the whole electrochemical system is in equilibrium, the charge transfer resistance can be found as in

$$R_{ct} = \frac{RT}{nFi_o} \tag{1}$$

1.3 Parasitic/Coating Capacitance (C_{par})

This capacitance variable is a general capacitance which is formed due to the separation of two conducting plates (reference and the working electrodes) by the non-conducting media (electrolyte solution) [11]. The mathematical relationship of this variable is shown below, as in

$$C_{par} = \frac{\varepsilon_o \varepsilon_r A}{d} \tag{2}$$

The impedance spectra and real-time impedance change induced on electrodes with different surface properties were successfully recorded [23]. The proposed impedance based sensor is the potential for further detection and quantification of cancer cells. In this research, the proposed equivalent circuit, significant variables and the experimental result of impedance measurement will be described in section II. In section III, the best electrode and frequency based on the existing data is selected. In-depth analysis and discussion for each stage of cell's invasive nature, the comparison between impedance measurement and the cell's resistance are explained in section III [13,25]. Section IV discloses all the related information and the conclusion.

2. Standard Growth Curve of Cancer Cell's Invasive Nature with the Proposed Equivalent Circuit Model

Making electrical impedance equivalent model in relation to the interface between electrode and electrolyte is of a great importance for sensory system [10]. The sensor based on impedance detection relys on monitoring of the electric impedance caused by the changes of the electrical current flow. The impedance data from experimental results can be analyzed and predicted by using proper electrical model [5]. In this work, a sensor system based on impedance using coplanar electrodes is investigated. The equivalent electrical circuit model with different parameters was implemented by using electromechanical systems [19].

These equivalent circuit models are designed to match each stage of the cell's invasion while the previous study as in research [11,17], the focus was on the general form of the cell's invasion nature. The resulting impedance and phase measurements were scattered and no standard pattern emerged. To overcome the limitations of this previous experiment, the equivalent circuit model, the output impedance versus time of ECIS measurement was categorized into 3 stages as shown in Fig. 1. Stage 1 (lag phase) occurs at the beginning where the electrode surface is uncovered. Then, Stage 2 (log phase) occurs when the electrode surface is covered by the cells. Finally, Stage 3 (stationary phase) occurs after cell manipulation. Refer Fig. 4, Fig. 7 and Fig. 10 in section III for more detail.

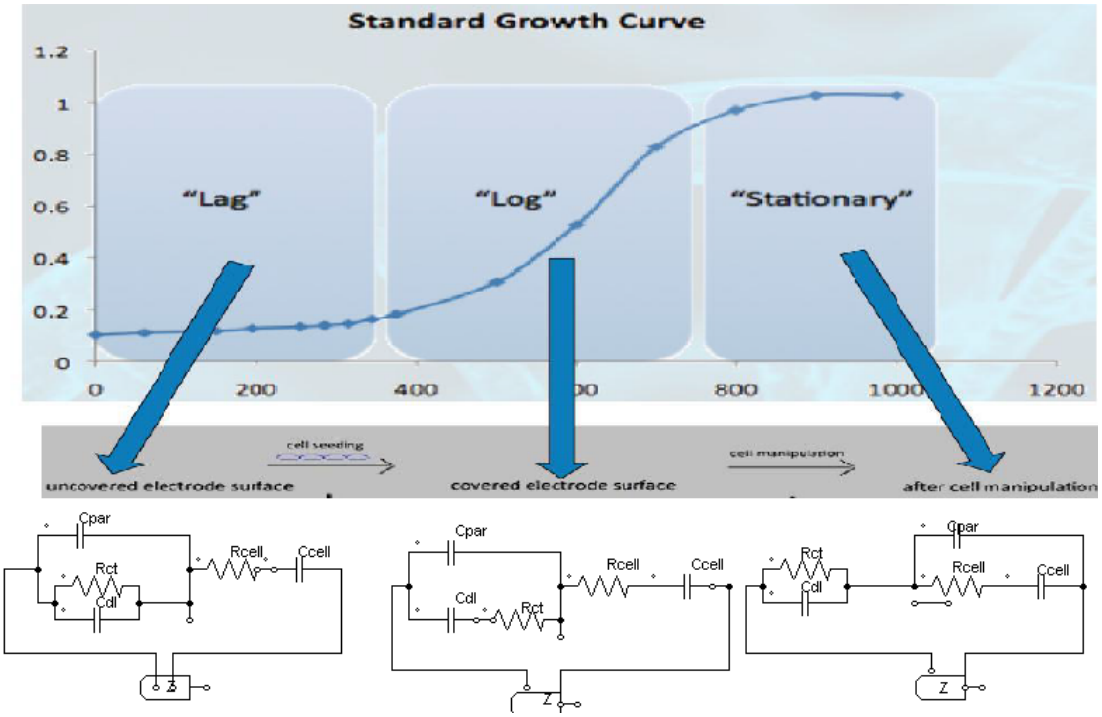

Fig. 1. The proposed equivalent circuit model represents each stage of the invasive nature

Significant Variables

2.1 Charge Transfer Resistance (R_{ct})

Eq. (1) is used to calculate this resistance. It is important to know that copper is the selected material for the biosensor design in the previous research [11,26].

Where: Gas Constant, R = 8.3145 J/molK, Temperature, T = 310 K.
Number of electrons, n = 2 (Cu^{2+} + $2e^{-}Cu$)
Faraday constant, F = 96485.3415 SA/mol
Exchange current density copper, i_o = 1 µAmm^{-2}
So, the value of charge transfer resistance is 48.1nΩ.
Coating/Parasitic Capacitance (C_{par})
Equation 2 is used to calculate this capacitance.
Where: Permittivity of free space, ε_o = 8.854 x 10^{-12} F/m Permittivity of material (DMEM),
ε_r = 80
Area of plate, A = 35µm x 6.1mm d: Depends on the electrode design (0.26mm is chosen) which is based on Table 1. So, the value of parasitic capacitance is 0.582µF.

Table 1
The value of the parasitic capacitance (Fairuzabadi)

Distance between Electrode, d (mm)	Parasitic Capacitance, C_{par} (µF)
0.26	0.582
0.53	0.285
0.80	0.189
1.06	0.143

2.2 Double Layer Capacitance (C_{dl})

Fairuzabadi [11] assumed the value of double layer capacitance is 1.22µF for this particular design.

Cell's Capacitance (C_{cell}).

One assumption needed to be made in order to successfully analyse the invasive nature of A549 cancer cell. The value of C_{cell} = 3.01µF is taken from previous research [11,34]. Since the value of cell's capacitance is insignificant in the long run. Even the value of cell's capacitance decreases as time goes on but the decrements are too small and minuscule. So, the cell's capacitance can be safely assumed to be constant throughout the analysis [7].

2.3 Impedance Measurement of A549 Lung Cancer Cell

The design and fabrication process of the biosensor, experimental setup, preparation of A549 lung cancer and impedance measurement from research [11] is incorporated in this study.

The impedance results from the research [11] are divided into two parts. The first part of the results in Table 2 shows the measurement for the 0.26mm electrode design at different range of frequencies.

Table 2
Graph for the 0.26mm electrode design at different Hz

Frequency (Hz)/Time (hours)	0	24	48	72	96	120
100	1644.89Ω	4055.00Ω	6223.23Ω	7682.75Ω	10527.17Ω	9712.54Ω
50k	149.62Ω	409.48Ω	444.00Ω	478.24Ω	517.12Ω	530.60Ω
1M	36.23Ω	41.90Ω	44.01Ω	46.9Ω	49.79Ω	51.96Ω
6M	33.25Ω	30.84Ω	30.39Ω	29.85Ω	28.72Ω	27.94Ω
10M	43.12Ω	41.15Ω	41.14Ω	41.44Ω	40.66Ω	39.79Ω

The Impedance For 0.26mm Electrode Design at Different Range of Frequencies [11]

The second part of the results in Table 3 show the measurements for all electrodes designs (0.26mm, 0.53mm, 0.80mm and 1.06mm) at 100 Hz.

Table 3
Graph for the 0.26mm electrode design at different Hz.

Design (mm)/Time (hours)	0	24	48	72	96	120
0.26	1644.89Ω	4055.00Ω	6223.23Ω	7682.75Ω	10527.17Ω	9712.54Ω
0.53	557.99Ω	2682.15Ω	5086.68Ω	7257.42Ω	9522.59Ω	6362.87Ω
0.80	73.40Ω	83.93Ω	70.70Ω	65.20Ω	275.46Ω	321.16Ω
1.06	53.99Ω	129.9Ω	101.79Ω	138.86Ω	117.22Ω	115.64Ω

The Impedance for All Electrode Design Ata100Hz [11]

3. Results and Discussions

3.1 The Best Electrode Design & the Best Frequency

Firstly, it is obvious that the best electrode design for analysing A549 lung cancer cell is the 0.26mm design (based on results from Table 3) and the best frequency to study the cell's invasive nature is at 100 Hz (based on results from Table 2). This is because the impedance measurement is highly accurate and precise at low frequency which is 100Hz. Furthermore, the narrower the distance between the electrodes, the more accurate the impedance measurement is. Besides that, the stages

of the cancer's invasive nature can be easily analysed by using suitable data analysis software [27,29]. Therefore, the discussion for each category of the invasive nature will be explained thoroughly in order to give a clear understanding of this research. Stage 1 is considered to be at 0 to 24 hours, Stage 2 is from 24 to 72 hours and Stage 3 is decided to be from 72 to 120 hours [3,14,26].

Results and Analysis for Stage 1 (0 - 24 hours).

The equivalent circuit model in Figure 2 will give the exact equation as the Eq. (3) (Equation |Z| for Stage 1). This equation needs a simple derivation to achieve Eq. 4 (Equation for R_{cell} for Stage 1).

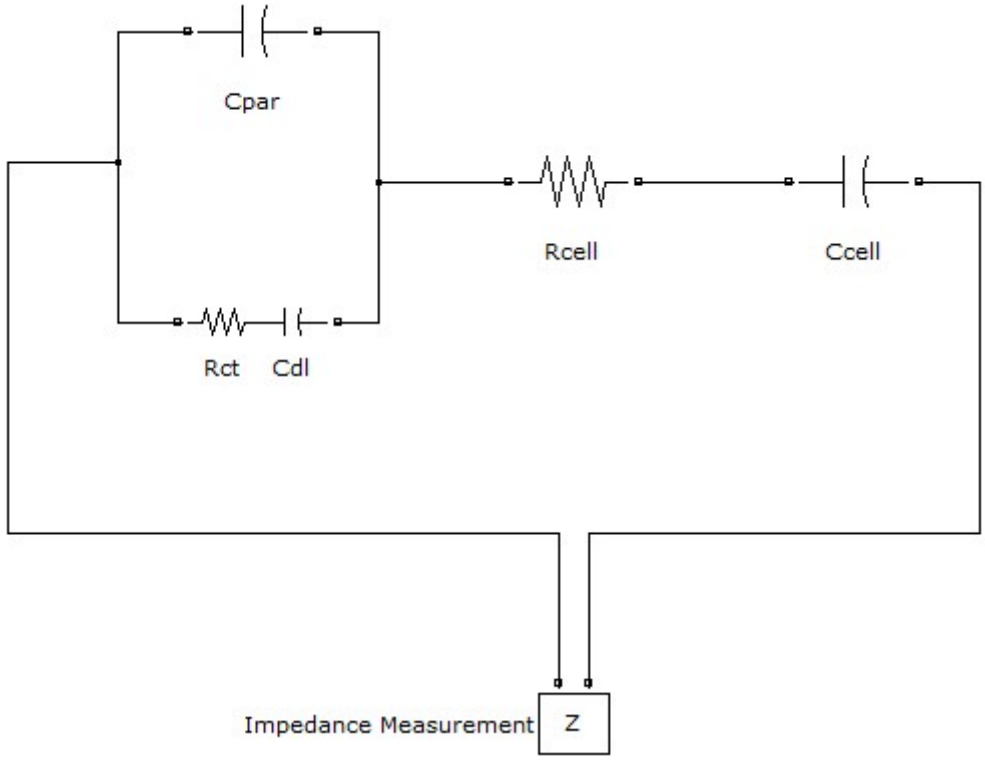

Fig. 2. The Proposed Equivalent Circuit Model for Stage 1

$$Z = X_{c_{par}} //(R_{ct} + X_{c_{dl}}) + R_{cell} + X_{c_{cell}} \quad (3)$$

The parameters needed to solve Equation 4 can be found by using information from section II (B), Table 1 and Table 2.

|Z| = 4055.00 - 1644.89 = 2410.11Ω
R_{ct} = 48.1nΩ
$X_{cdl} = 1/ (2\pi f C_{dl}) = 1/ [(200\pi) (1.22\mu F)] = 1304.549\Omega$
$X_{cpar} = 1/ (2\pi f C_{par}) = 1/ [(200\pi) (0.582\mu F)] = 2734.621\Omega$
$X_{ccell} = 1/ (2\pi f C_{cell}) = 1/ [(200\pi) (3.01\mu F)] = 528.754\Omega$

Consequently, the value of R_{cell} is 998Ω. Then, using the data analysis software such as EIS Spectrum Analyzer, MATLAB Powergui and Simulink, the results are shown in the following Figure 3 and Figure 4.

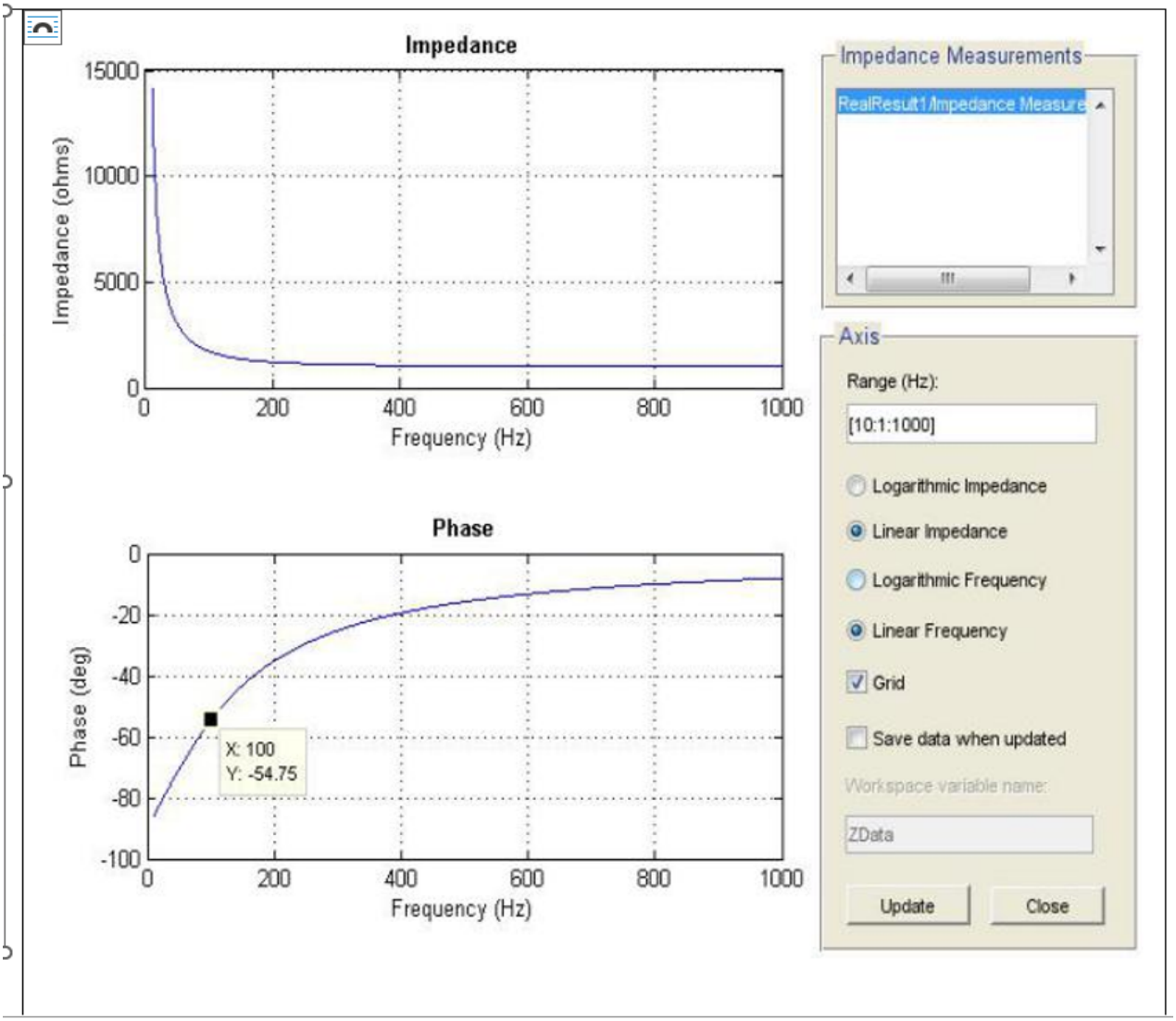

Fig. 3. Matlab Powergui and Simulink data analysis for Stage 1

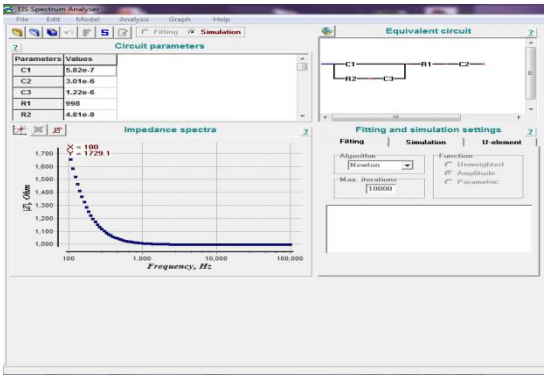

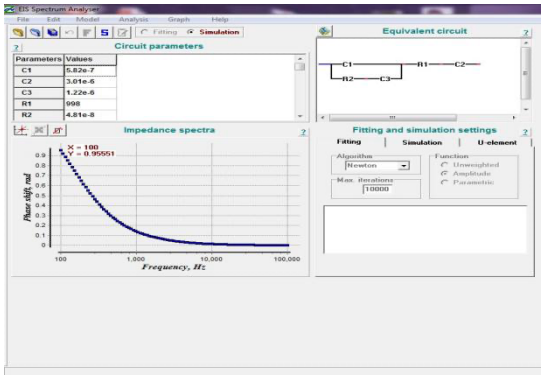

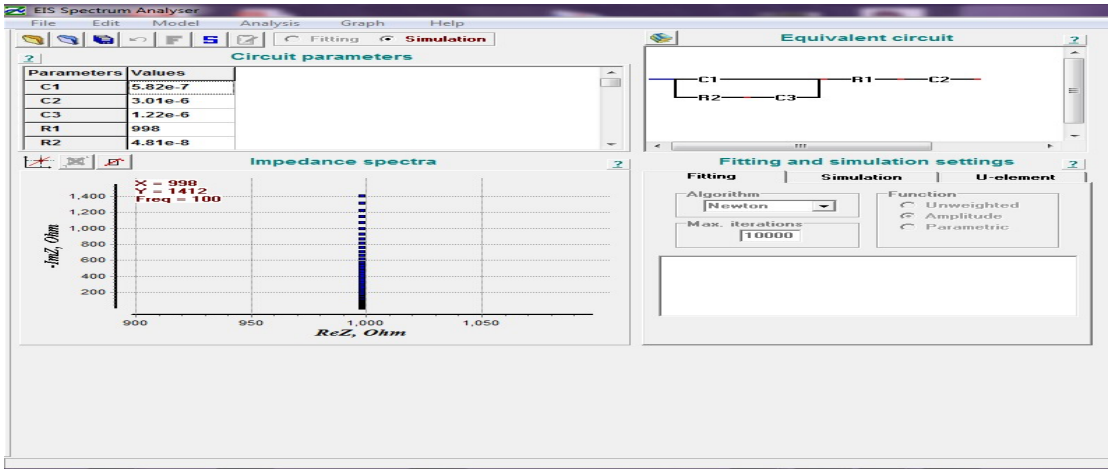

Fig. 4. EIS Spectrum Analyzer data analysis for Stage 1

Results and Analysis for Stage 2 (24 - 72 hours) The equivalent circuit model in Figure 5 will give the exact equation as the Eq. (5) (Equation |Z| for Stage 2). This equation needs a simple derivation to achieve Eq. (6) (Equation for R_{cell} for Stage 2).

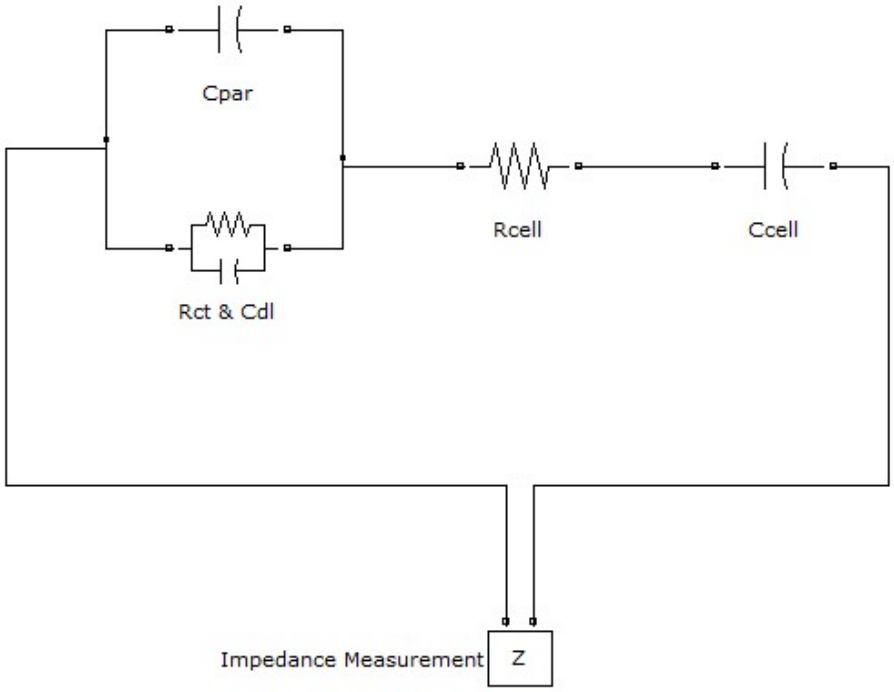

Fig. 5. The Proposed Equivalent Circuit Model for Stage 2

$$Z = X_{c_{par}} //(R_{ct} // X_{c_{dl}}) + R_{cell} + X_{c_{cell}} \tag{5}$$

$$R_{cell} = Z - X_{c_{cell}} - \frac{X_{c_{par}} \dfrac{R_{ct} X_{c_{dl}}}{R_{ct} + X_{c_{dl}}}}{X_{c_{par}} + \dfrac{R_{ct} X_{c_{dl}}}{R_{ct} + X_{c_{dl}}}} \tag{6}$$

The parameters needed to solve Eq. (6) [27] can be found by using information from section II (B), Table 1 & Table 2.

$|Z|$ = 7682.75 - 4055.00 = 3627.75Ω
R_{ct} = 48.1nΩ $X_{cdl} = 1/ (2\pi f C_{dl}) = 1/ [(200\pi) (1.22\mu F)] = 1304.549\Omega$
$X_{cpar} = 1/ (2\pi f C_{par}) = 1/ [(200\pi) (0.582\mu F)] = 2734.621\Omega$
$X_{ccell} = 1/ (2\pi f C_{cell}) = 1/ [(200\pi) (3.01\mu F)] = 528.754\Omega$The value of R_{cell} is 3099Ω.

Then, by using the data analysis software EIS Spectrum Analyzer, MATLAB Powergui and Simulink, the results are shown in the following Figure 6 and Figure 7.

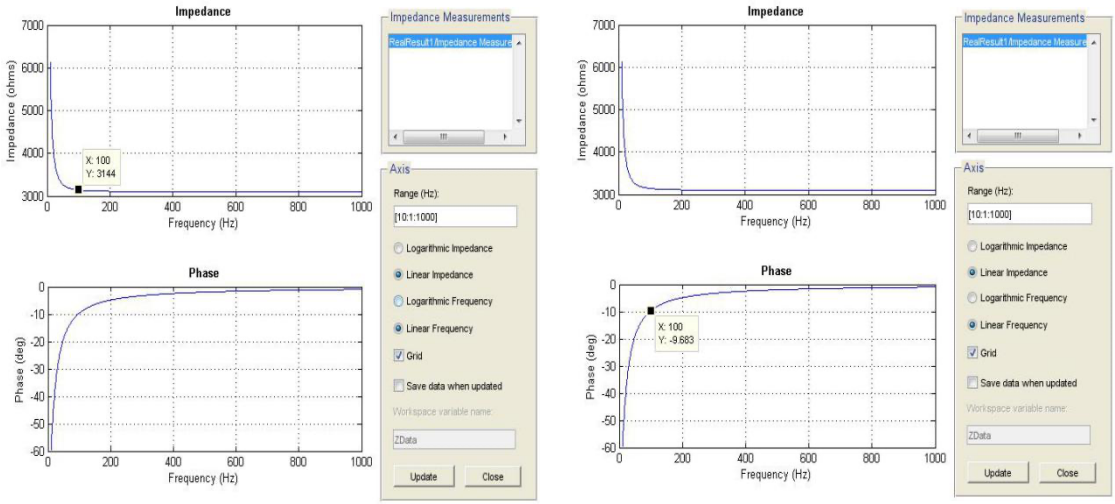

Fig. 6. Matlab Powergui and Simulink data analysis for Stage 2

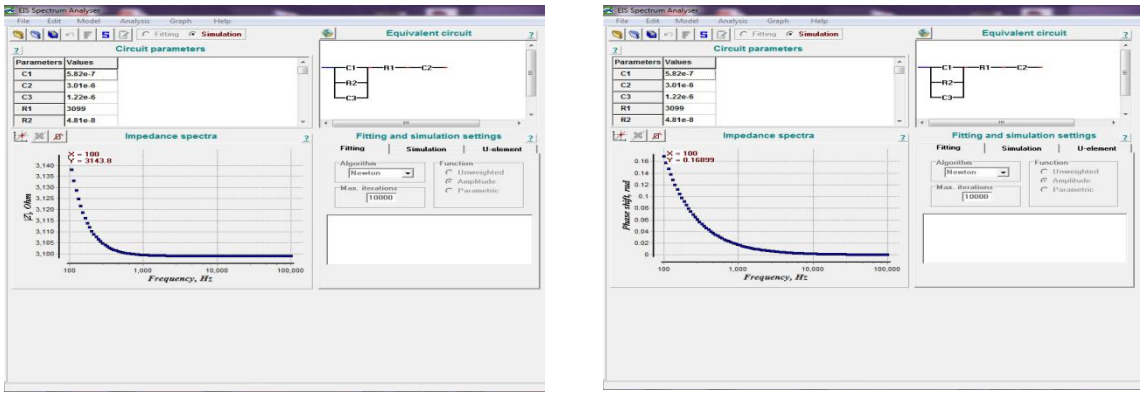

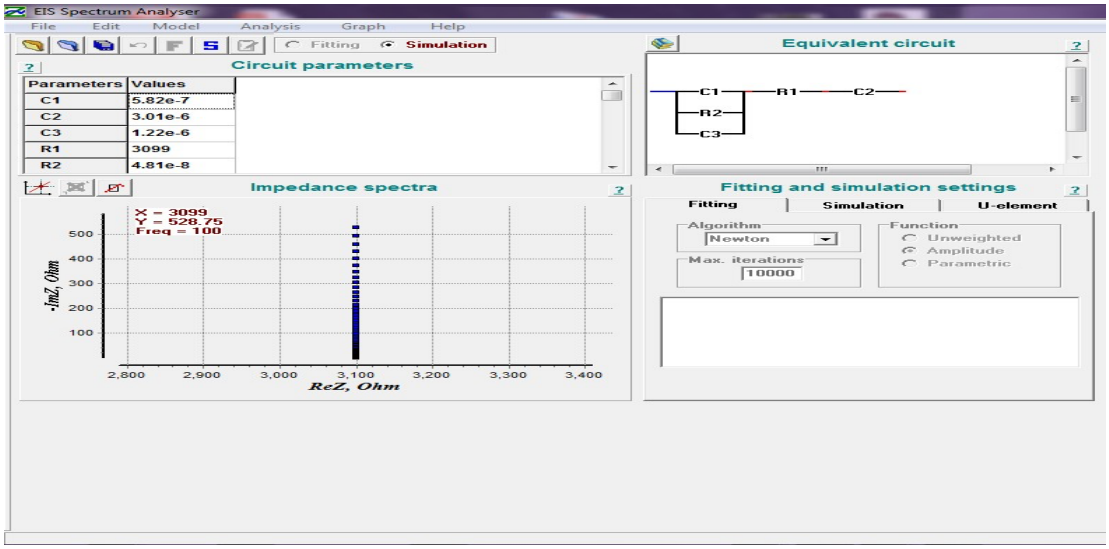

Fig. 7. EIS Spectrum Analyzer data analysis for Stage 2

Results and Analysis for Stage 3 (72 - 120 hours). The equivalent circuit model in Figure 8 will give the exact equation as the Eq. (7) (Equation |Z| for Stage 3) while this equation needs a simple derivation to achieve Eq. (8) (Equation for R_{cell} for Stage 3).

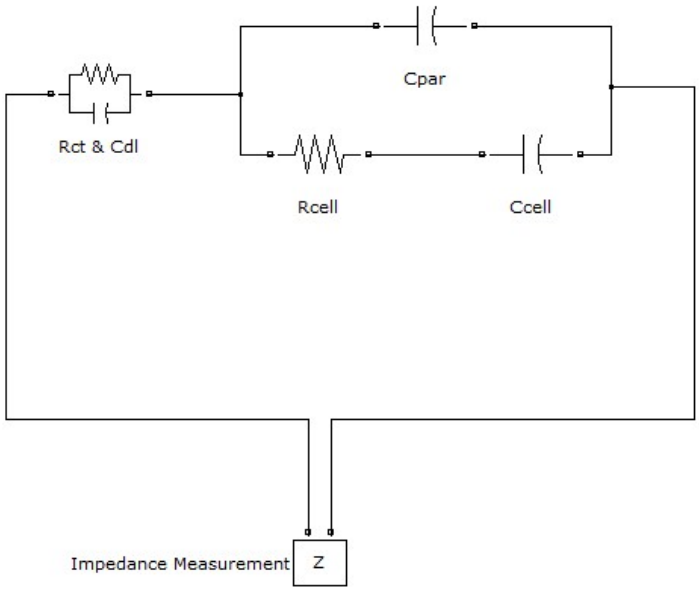

Fig. 8. The Proposed Equivalent Circuit Model for Stage 3

$$Z = (R_{ct} // X_{c_{dl}}) + X_{c_{par}} // (R_{cell} + X_{c_{cell}}) \tag{7}$$

$$R_{cell} = \frac{X_{c_{par}} X_{c_{cell}} - (X_{c_{par}} + X_{c_{cell}})(Z - \frac{R_{ct} X_{c_{dl}}}{R_{ct} + X_{c_{dl}}})}{Z - \frac{R_{ct} X_{c_{dl}}}{R_{ct} + X_{c_{dl}}} - X_{c_{par}}} \tag{8}$$

As expected, the parameters needed to solve Eq. (8) can be found by using information from section II (B), Table 1 & Table 2.

$|Z| = 9712.54 - 7682.75 = 2029.79\Omega$ $R_{ct} = 48.1n\Omega$
$X_{cdl} = 1/ (2\pi fC_{dl}) = 1/ [(200\pi) (1.22\mu F)] = 1304.549\Omega$
$X_{cpar} = 1/ (2\pi fC_{par}) = 1/ [(200\pi) (0.582\mu F)] = 2734.621\Omega$
$X_{ccell} = 1/ (2\pi fC_{cell}) = 1/ [(200\pi) (3.01\mu F)] = 528.754\Omega$

Therefore, the value of R_{cell} is 7346Ω. Then, by using the data analysis software EIS Spectrum Analyzer, MATLAB Powergui and Simulink, the results are shown in the following Figure 9 and Figure 10.

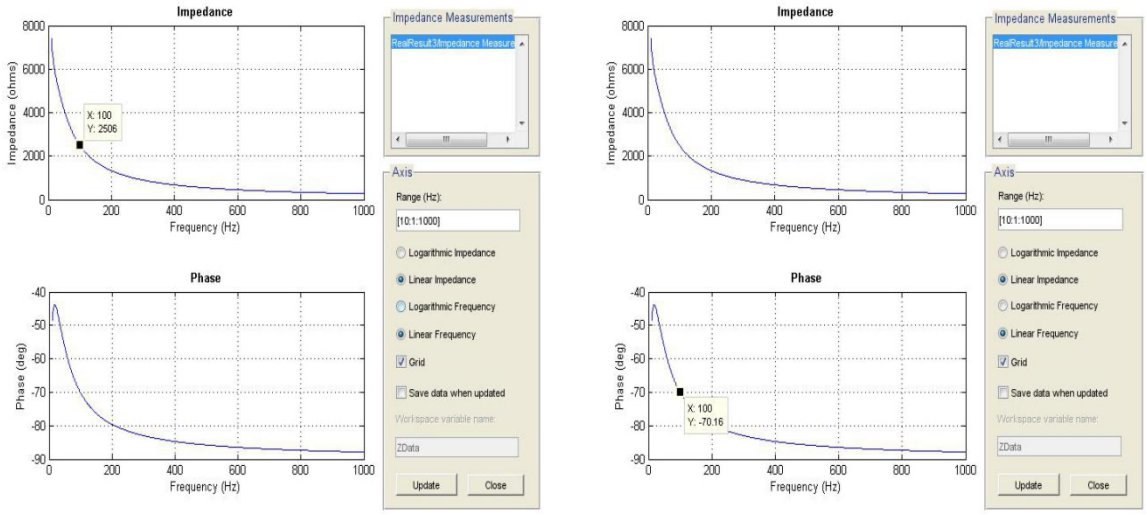

Fig. 9. Matlab Powergui and Simulink data analysis for Stage 3

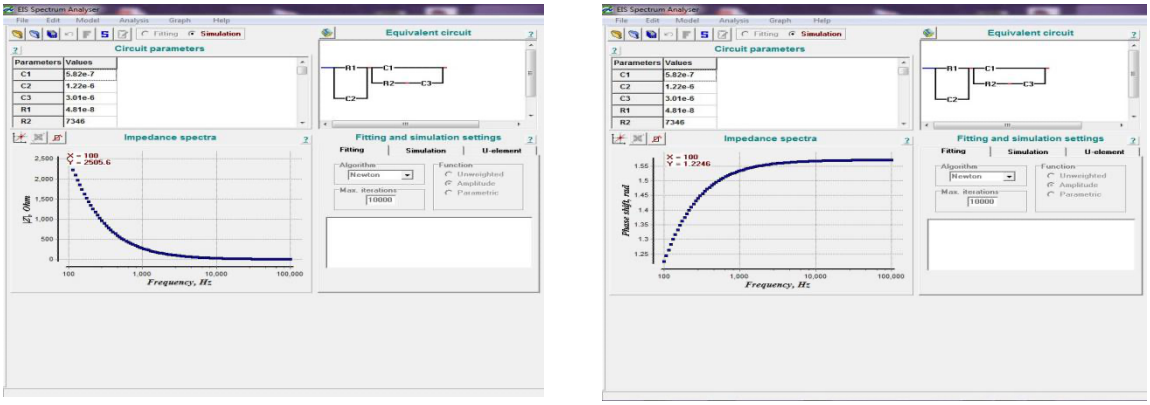

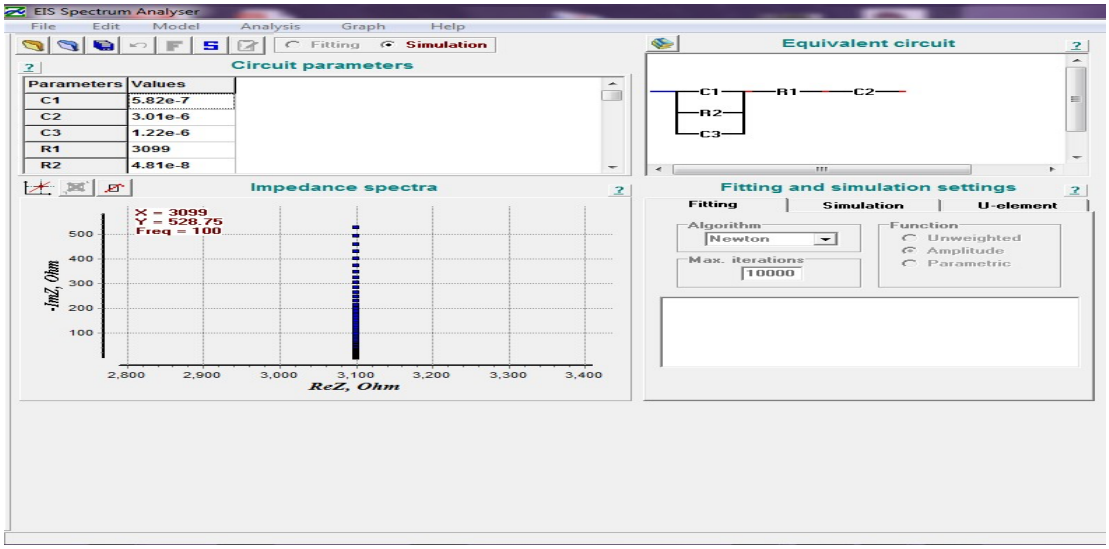

Fig. 10. EIS Spectrum Analyzer data analysis for Stage 3

4. Discussion for Each Stage

In Figure 3, Figure 6 and Figure 9, the MATLAB Powergui and Simulink software displays the values in linear impedance and linear frequency for each stage which are shown below:

i. Stage 1 |Z| = 1729Ω Phase Shift = -54.75°
ii. Stage 2 |Z| = 3144Ω Phase Shift = -9.683°
iii. Stage 3 |Z| = 2506Ω Phase Shift = -70.16°

Meanwhile, the EIS Spectrum Analyzer software displays three values in Figure 4, Figure 7 and Figure 10 that has one extra component for each stage:

i. Stage 1
|Z| = 1729.1Ω Phase Shift = 0.95551rad / 54.75° Real part, R_s = 998Ω, Imaginary part, X_s = 1412Ω
ii. Stage 2
|Z| = 3143.8Ω Phase Shift = 0.16899rad / 9.682° Real part, R_s = 3099Ω, Imaginary part, X_s = 528.75Ω
iii. Stage 3
|Z| = 2505.6Ω Phase Shift = 1.2246rad / 70.16° Real part, R_s = 850.2Ω, Imaginary part, X_s = 2356.9Ω

If we observe carefully, the values of impedance measurement, |Z| and phase shift are extremely similar in each stage for all the software [14,34]. However, there is a major difference in the polarity of phase shift's values. In Matlab Powergui and Simulink software, the polarity of the phase shift is negative while in EIS Spectrum Analyzer the polarity of the phase shift is positive. In addition, the EIS Spectrum Analyzer has successfully determined the real part and the imaginary part of the impedance value |Z| in each stage, while the Matlab Powergui and Simulink are unable to separate the real and imaginary component.

4.1 Comparison of Impedance Measurement

It is crucial to compare the actual reading of the impedance measurements with the EIS Spectrum Analyzer and MATLAB Powergui and Simulink in order to verify the analytical power of these softwares [17]. The analysis is shown below in Table 4 and Figure 11.

Table 4
The impedance measurement from the actual reading with different software

Stages of Lung Cancer's Invasive Nature	Actual Reading (Ω)	EIS Spectrum Analyzer (Ω)	Matlab Powergui and Simulink (Ω)
1	2410.11	1729.10	1729.00
2	3627.75	3143.80	3144.00
3	2029.79	2505.60	2506.00

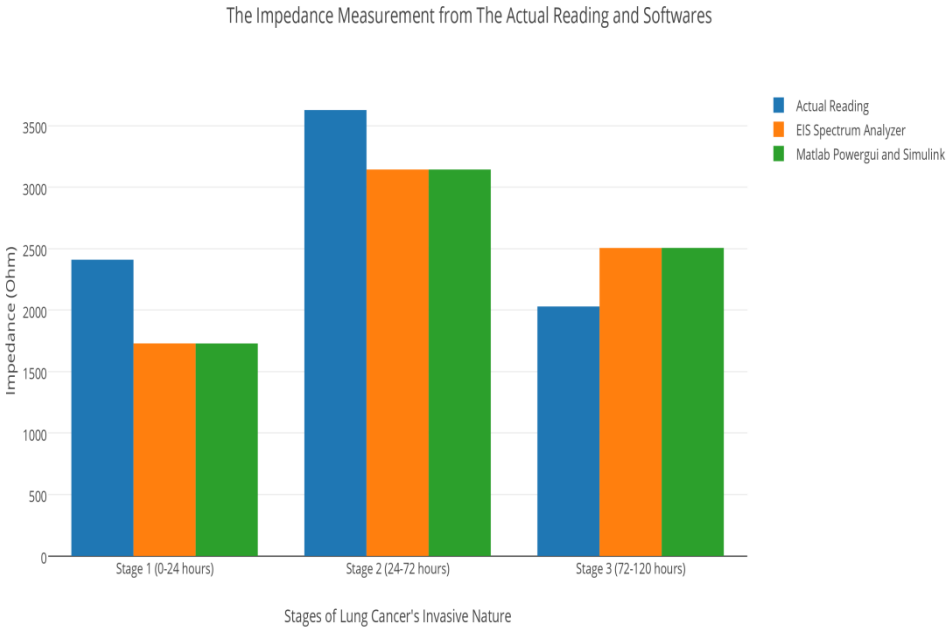

Fig. 11. Bar graph comparing the impedance measurements between the actual reading and the software

The following calculation shows the percentage errors for impedance measurements recorded by both software compared to the actual reading in each stage.

i. % Error of Stage 1
EIS Spectrum Analyzer
% Error = |(1729.10 - 2410.11) / (2410.11)| x 100% = 28.2564%
Matlab Powergui and Simulink
% Error = |(1729.00 - 2410.11) / (2410.11)| x 100% = 28.2605%

ii. % Error of Stage 2
EIS Spectrum Analyzer
% Error = |(3143.80 - 3627.75) / (3627.75)| x 100% = 13.3402%
Matlab Powergui and Simulink % Error = |(3144.00 - 3627.75) / (3627.75)| x 100% = 13.3347%

iii. % Error of Stage 3

EIS Spectrum Analyzer % Error = |(2505.60 - 2029.79) / (2029.79)| x 100% = 23.4413%
Matlab Powergui and Simulink % Error = |(2506.00 - 2029.79) / (2029.79)| x 100% = 23.4610%

Based on the data above, it is safe to assume that the percentage errors of both software are less than 30% which is quite high from the actual reading of the impedance measurement. Probably, the above software tools are not suitable to analyse the impedance value of A549 lung cancer cell but are suitable for other purposes such as determining the real part (R_s) and imaginary part (X_s) of the impedance value |Z| that has been stated in the previous discussion in section III (E).

4.2 Analysis and Discussion for Cell's Resistance

The investigated model has strong predictive abilities since it accurately predicts cellular actions and reactions in a range of experimental settings. It provides exploratory insights that enable researchers to investigate settings that are difficult to replicate in the lab. The model also facilitates hypothesis production, offering an important tool for developing hypotheses.

The model does have drawbacks, though. It frequently calls for simplifications and assumptions due to the limitations of present knowledge and computers. It is difficult to validate, and this could lead to discrepancies between model predictions and actual observations because of unaccounted-for interactions. The last and the most crucial part of the analysis and discussion is to discover the invasive nature of the lung cancer cell. It is going to be a spectacular discovery if there is any recognizable pattern in the cell's resistance. Based on the previous analysis in Section III (B, C & D), the value of R_{cell} is arranged in Table 5 below and can be plotted by using Plotly which is shown in the following Figure 12.

Table 12
The value of Rcell in each stage

Stages of Lung Cancer's Invasive Nature		1	2	3
Resistance of Lung Cancer's Cell,	Rcell (Ω)	998	3099	7346

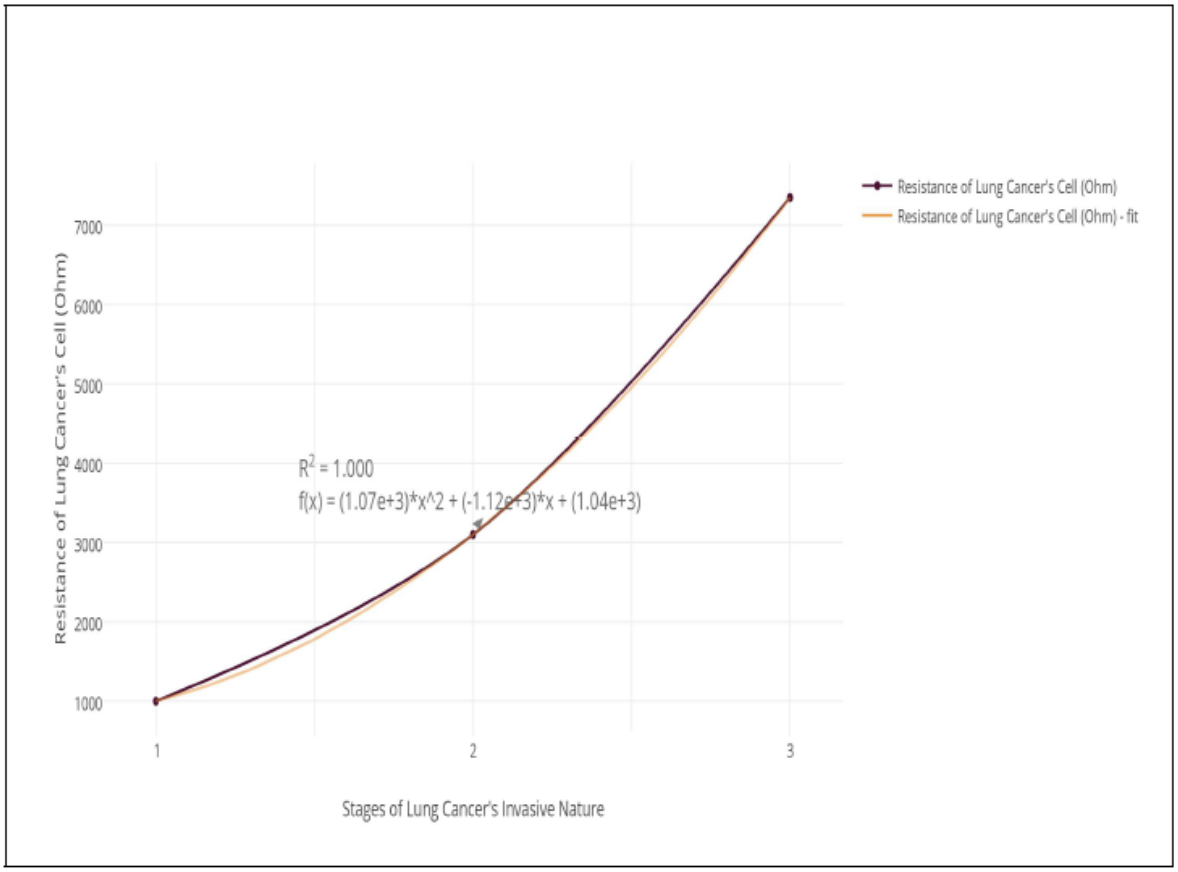

Fig. 12. Line graph for the value of R_{cell} in each stage

Surprisingly, the value R_{cell} in each stage from Figure 12 is best described by the quadratic equation as shown in Equation 9 (Quadratic equation for the value of R_{cell}).

$$f(x) = 1070x^2 - 1120x + 1040 \tag{9}$$

Where f(x) is the value of A549 lung cancer cell's resistance, R_{cell} and variable x can be referred as the stages of the cancer's invasive nature. In fact, by applying the concept of polynomial regression in Plotly, the best fit line and the value of R^2 are easily obtained. The value of R^2 is 1.000 and the best fit line is extremely similar to the actual data. Hence, Eq. (9) is definitely reliable and can be used to predict the value of R_{cell} in order to understand the nature of the A549 lung cancer cell. Now days, cancer is one of the major killer diseases in many countries where different treatments including Chemotherapy are applied. In preclinical testing studies, it is necessary to develop more rapid and simpler techniques for detection of cancerous cells, especially for understanding their interaction with drugs and toxins. Current methods that are used in cancer detection and treatment include techniques that usually need complex experimental process in inflexible laboratory conditions, as well as measurement methods that are costly. Also, these are not suitable for monitoring the sample continuously, and as a result, the data collected may not present the real changes in the cell activities at a specific time. Proposed impedance type cancer detector presents minimally invasive, reliable, inexpensive and easy to use measurement system that can be frequently used. Design in the Integration: Create a paradigm that supports experimental design. This could entail predicting the best experimental circumstances, such as medium compositions, measurement times, or appropriate controls, using the model. The research process might be streamlined with such integration. To

improve the model's forecasting skills, investigate the integration of machine learning approaches. Work together with physicians and experimental biologists to compare the model's predictions to actual data.

5. Conclusion

This investigation on A549 lung cancer cells is multifaceted and includes various stages. The normative behaviour of these cells was initially in-depth analysed, using knowledge gained from prior research data. The study then made use of the potential of an equivalent circuit model that had been carefully created to include simplicity without sacrificing effectiveness. Impedance measurements were used with this model to give specific information on the cellular phases that characterise the invasive nature of lung cancer. The deliberate use of cutting-edge data analysis tools, such as Matlab Powergui and Simulink, EIS Spectrum Analyser, and Plotly, was essential to this project. These tools worked in concert with a strict mathematical framework to make it easier to understand the shape of A549 lung cancer cells. A novel equation capable of predicting the cell's resistance as it changes phases was created from this research, which is a very notable finding. A crucial development is the establishment of a quadratic equation that controls the cell's resistance. This equation not only improves our comprehension of cellular dynamics but also provides a reliable indicator of the increasing resistance shown by A549 lung cancer cells as they go through the phases of the disease. In summary, this study accomplishes its goals while also laying the groundwork for a better understanding of cellular behaviour in relation to the development of lung cancer.

Acknowledgement
This research was not funded by any grant.

References

[1] Alshareef, A., Pandit, S., Hasan, M. N., et al. (2019). Electrical cell-substrate impedance sensing (ECIS) as a non-invasive monitoring tool for evaluating cell adhesion. Journal of Visualized Experiments, (143), e59070.

[2] Bai, Y., Liu, L., Li, X., et al. (2021). 3D-printed microfluidic chips for cancer research: current status and future directions. Micromachines, 12(5), 564.

[3] Benoy, Elizabeth C. "Influence of Fibroblasts on Metastatic Cancer Cell Drug Resistance in a 3D Microfluidic Cell Array." (2017).

[4] Bohunicky, B. and Mousa, S.A., 2010. Biosensors: the new wave in cancer diagnosis. *Nanotechnology, science and applications*, pp.1-10.

[5] Braunhut, Susan J., Donna McIntosh, Ekaterina Vorotnikova, Tiean Zhou, and Kenneth A. Marx. "Detection of apoptosis and drug resistance of human breast cancer cells to taxane treatments using quartz crystal microbalance biosensor technology." *Assay and Drug Development Technologies* 3, no. 1 (2005): 77-88.

[6] Cai, H., Zhang, Y., Liu, X., et al. (2021). Non-invasive evaluation of anti-cancer effects using electric cell-substrate impedance sensing (ECIS) system. International Journal of Nanomedicine, 16, 2865-2876.

[7] Chen, D. I., Weijie Guo, Zhaoping Qiu, Qifeng Wang, Yan Li, Linhui Liang, Li Liu, Shenglin Huang, Yingjun Zhao, and Xianghuo He. "MicroRNA-30d-5p inhibits tumour cell proliferation and motility by directly targeting CCNE2 in non-small cell lung cancer." *Cancer letters* 362, no. 2 (2015): 208-217.

[8] Chen, X., Chen, Y., Zheng, J., et al. (2020). A non-invasive cell impedance biosensor for monitoring breast cancer cell migration. Talanta, 209, 120548.

[9] Chen, Y., Huang, J., Wang, J., et al. (2021). Non-invasive lung cancer detection using impedimetric sensor array based on 3D printed electrode. Sensors and Actuators B: Chemical, 329, 129232.

[10] Cheng, Shan, Tracey A Martin, Xu Teng, and Wen G Jiang. "Putative Breast Tumor Suppressor TACC2 Suppresses the Aggressiveness of Breast Cancer Cells through a PLC Pathway." *Current Signal Transduction Therapy* 6, no. 1 (2011): 55-64.

[11] FAIRUZABADI, A. 2013. Development of an impedance based biosensor for characterization of cancer cells (Undergraduate). *International Islamic University Malaysia.*

[12] Feng, L., Li, Y., He, Y., et al. (2020). In vitro lung cancer detection by a fiber-optic impedimetric sensor based on aptamer-functionalized graphene oxide. Sensors and Actuators B: Chemical, 320, 128335.
[13] Finkel, Toren, Manuel Serrano, and Maria A. Blasco. "The common biology of cancer and ageing." *Nature* 448, no. 7155 (2007): 767-774.
[14] Franks, Wendy, Iwan Schenker, Patrik Schmutz, and Andreas Hierlemann. "Impedance characterization and modeling of electrodes for biomedical applications." *IEEE Transactions on Biomedical Engineering* 52, no. 7 (2005): 1295-1302.
[15] Gazdar, Adi F., Luc Girard, William W. Lockwood, Wan L. Lam, and John D. Minna. "Lung cancer cell lines as tools for biomedical discovery and research." *Journal of the National Cancer Institute* 102, no. 17 (2010): 1310-1321.
[16] Giaever, Ivar, and Charles R. Keese. "Electric cell-substrate impedance sensing concept to commercialization." In *Electric cell-substrate impedance sensing and cancer metastasis*, pp. 1-19. Dordrecht: Springer Netherlands, 2012.
[17] Hong, Jongin, Karthikeyan Kandasamy, Mohana Marimuthu, Cheol Soo Choi, and Sanghyo Kim. "Electrical cell-substrate impedance sensing as a non-invasive tool for cancer cell study." *Analyst* 136, no. 2 (2011): 237-245.
[18] Jiang, Wen G., ed. *Electric cell-substrate impedance sensing and cancer metastasis*. Vol. 17. Springer Science & Business Media, 2012.
[19] Jiang, Wen G., Lin Ye, Fiona Ruge, Ping-Hui Sun, Andrew J. Sanders, Ki Ji, Jane Lane et al. "Expression of Sonic Hedgehog (SHH) in human lung cancer and the impact of YangZheng XiaoJi on SHH-mediated biological function of lung cancer cells and tumor growth." *Anticancer research* 35, no. 3 (2015): 1321-1331.
[20] Keese, Charles R., Kaumudi Bhawe, Joachim Wegener, and Ivar Giaever. "Real-time impedance assay to follow the invasive activities of metastatic cells in culture." *Biotechniques*33, no. 4 (2002): 842-850.
[21] Li, Y., Li, Y., Li, M., et al. (2019). Microfluidic platforms for cancer diagnosis. Biosensors and Bioelectronics, 141, 111416.
[22] Li, Y., Xu, F., Yan, Q., et al. (2020). Electrospun PCL/PLA composite nanofibers for three-dimensional culture of lung cancer cells. ACS Biomaterials Science & Engineering, 6(6), 3401-3411.
[23] Liu, Qingjun, Jinjiang Yu, Lidan Xiao, Johnny Cheuk On Tang, Yu Zhang, Ping Wang, and Mo Yang. "Impedance studies of bio-behavior and chemosensitivity of cancer cells by micro-electrode arrays." *Biosensors and Bioelectronics* 24, no. 5 (2009): 1305-1310.
[24] Liu, Y., Zhao, X., Zhang, Z., et al. (2022). In situ and real-time monitoring of cellular dynamics by impedance sensing with adjustable sensitivity. ACS Sensors, 7(3), 878-887.
[25] Maher, J., and H. McConnell. "New pathways of care for cancer survivors: adding the numbers." *British Journal of Cancer* 105, no. 1 (2011): S5-S10.
[26] Mamouni, Jaouad, and Liju Yang. "Interdigitated microelectrode-based microchip for electrical impedance spectroscopic study of oral cancer cells." *Biomedical microdevices* 13 (2011): 1075-1088.
[27] Mansor, Ahmad Fairuzabadi Mohd, Anis Nurashikin Nordin, and Irmanisha Ibrahim. "Cytotoxicity studies of lung cancer cells using impedance biosensor." In *2015 International Conference on Smart Sensors and Application (ICSSA)*, pp. 1-6. IEEE, 2015.
[28] Nguyen, Tien Anh, Tsung-I. Yin, and Gerald Urban. "A cell impedance sensor chip for cancer cells detection with single cell resolution." In *SENSORS, 2013 IEEE*, pp. 1-4. IEEE, 2013.
[29] Nguyen, Tien Anh, Tsung-I. Yin, Diego Reyes, and Gerald A. Urban. "Microfluidic chip with integrated electrical cell-impedance sensing for monitoring single cancer cell migration in three-dimensional matrixes." *Analytical chemistry* 85, no. 22 (2013): 11068-11076.
[30] Price, Dorielle T. *Optimization of Bio-Impedance Sensor for Enhanced Detection and Characterization of Adherent Cells*. University of South Florida, 2012.
[31] Qiao, Y., Wang, Y., Zhang, J., et al. (2019). A highly sensitive electrochemical biosensor for lung cancer cell detection based on platinum nanoclusters-graphene oxide hybrids. Biosensors and Bioelectronics, 135, 1-8.
[32] Siddiquei, H. R., A. N. Nordin, M. I. Ibrahimy, M. A. Arifin, N. H. Sulong, M. Mel, and I. Voiculescu. "Electrical cell-substrate impedance sensing (ECIS) based biosensor for characterization of DF-1 cells." In *International Conference on Computer and Communication Engineering (ICCCE'10)*, pp. 1-4. IEEE, 2010.
[33] Song, H., Zhang, C., Yao, C., et al. (2020). A label-free electrochemical impedance biosensor based on the polypyrrole/ionic liquid/graphene oxide nanocomposite for detection of lung cancer cells. Talanta, 207, 120311.
[34] Walker, Glenn M., and David J. Beebe. "A passive pumping method for microfluidic devices." *Lab on a Chip* 2, no. 3 (2002): 131-134.
[35] Erickson, David, and Dongqing Li. "Integrated microfluidic devices." *Analytica chimica acta* 507, no. 1 (2004): 11-26.
[36] Wei, X., He, X., Wang, K., et al. (2021). Gold nanoparticle-decorated carbon nanofiber arrays for electrochemical impedance biosensing of cancer cells. Analytica Chimica Acta, 1176, 338620.

[37] Yang, Y., Zheng, J., He, Y., et al. (2021). PEG-based hydrogels for 3D lung cancer cell culture and drug screening. Journal of Materials Chemistry B, 9(7), 1768-1778.
[38] Zhang, X., Li, J., Xu, S., et al. (2020). Engineering hydrogel microenvironments for cancer modeling and drug testing. Journal of Materials Chemistry B, 8(43), 9779-9791.